ISSN 1440-771X

MONASH University

Department of Econometrics and Business Statistics

http://www.buseco.monash.edu.au/depts/ebs/pubs/wpapers/

# Description Length and Dimensionality Reduction in Functional Data Analysis

D. S. Poskitt and A. Sengarapillai

November 2009

Working Paper 13/2009

# Description Length and Dimensionality Reduction in Functional Data Analysis

**D. S. Poskitt**
Department of Econometrics and Business Statistics,
Monash University,
VIC 3800
Australia.
Email: don.poskitt@buseco.monash.edu.au

**A. Sengarapillai**
Department of Mathematics and Statistics,
University of Jaffna,
SriLanka.
Email: arivu90@gmail.com

12 November 2009

**JEL classification:** C14,C22

# Description Length and Dimensionality Reduction in Functional Data Analysis

**Abstract:** In this paper we investigate the use of description length principles to select an appropriate number of basis functions for functional data. We provide a flexible definition of the dimension of a random function that is constructed directly from the Karhunen–Loève expansion of the observed process. Our results show that although the classical, principle component variance decomposition technique will behave in a coherent manner, in general, the dimension chosen by this technique will not be consistent. We describe two description length criteria, and prove that they are consistent and that in low noise settings they will identify the true finite dimension of a signal that is embedded in noise. Two examples, one from mass-spectroscopy and the one from climatology, are used to illustrate our ideas. We also explore the application of different forms of the bootstrap for functional data and use these to demonstrate the workings of our theoretical results.

**Keywords:** Bootstrap, consistency, dimension determination, Karhunen–Loève expansion, signal-to-noise ratio, variance decomposition.

# 1 Introduction

In the analysis of functional data, wherein each observation is a curve or image, it is commonly supposed that the random curves or functions $X$ are sampled from a stochastic process in $\mathcal{L}^2_{[0,\tau]}$. Here, $\mathcal{L}^2_{[0,\tau]}$ is the Hilbert space of square integrable functions on the interval $[0,\tau]$, with inner product $< f, g >= \int_0^\tau f(t)g(t)dt$ for any two functions $f, g \in \mathcal{L}^2_{[0,\tau]}$ and induced squared norm $\| \cdot \|^2 =< \cdot, \cdot >$. A Karhunen–Loève expansion of $X$ is also assumed to exist such that

$$X(t) = \mu(t) + \sum_{j=1}^{\infty} \xi_j \, \rho_j(t), \tag{1}$$

where the mean function $\mu(t) = E[X(t)]$ and the basis functions $\rho_j(t)$ are the orthonormal eigenfunctions of the covariance kernel $\Gamma(s,t) = Cov[X(s), X(t)]$. The eigenvalues corresponding to the $\rho_j(t)$ are listed in decreasing order, so that, without loss of generality, $\lambda_1 > \lambda_2 > \cdots$, where $\int_0^\tau \Gamma(s,t)\rho_j(t)dt = \lambda_j \rho_j(s)$ and

$$\Gamma(t,s) = \sum_{j=1}^{\infty} \lambda_j \rho_j(t) \rho_j(s) \, . \tag{2}$$

The coefficients $\xi_j$ are given by the projection of $X - \mu$ in the direction of the jth eigenfunction $\rho_j$, *i.e.* $\xi_j =< X - \mu, \rho_j >$. The $\xi_j$ constitute an uncorrelated sequence of random variables with zero mean and variance $\lambda_j$, and since the process $X$ lies in $\mathcal{L}^2_{[0,\tau]}$ we have $\sum_{j=1}^{\infty} \lambda_j < \infty$. The monographs by Ramsay and Silverman (1997, 2002) present original expositions of various aspects of functional data analysis, see also Ferraty and Vieu (2006) and the references contained therein.

Although the series expansions in equations (1) and (2) are infinite dimensional, it is often found that a given functional data set can effectively be spanned by $k \ll \infty$ basis functions. Truncating the expansions after $k$ terms and expressing the functions in terms of a low dimensional, finite basis offers considerable practical advantages, not least because it allows various techniques of multivariate statistical analysis to be applied with little or no adaptation. Asymptotic analyses of random samples of $X$ are commonly predicated on the assumption that the truncation point $k \to \infty$ as the number of sampled curves, $n$, increases, see, *inter alia*, Yao et al. (2005) and Hall et al. (2006). In practical applications, however, $k$ is always finite and must be chosen by reference to the data. It is the choice of $k$ that is the main focus of this paper.

Various approaches to selecting $k$ can be contemplated (Ramsay and Silverman, 1997, Section 4.5), but it is an open question as to how conventional dimension reduction methods can be adapted to the infinite dimensional setting of functional data (Ferraty and Vieu, 2006, Section 6.4). To the current authors' knowledge there is little in the current literature that explicitly investigates the theoretical properties of dimension reduction techniques within a functional framework. A notable exception is the work by Hall and Vial (2006), that builds upon the theoretical results presented in Hall and Hosseini-Nasab (2006). Hall and Vial assume a signal-plus-noise model for the observed process and consider determining $k$ by examining the null hypothesis that the signal has fewer than $k$ dimensions. They show that for such a model the noise will be confounded with the signal, and suggest that the intrinsic impossibility of estimating the full extent of the noise that results from this confounding means that conventional hypothesis testing techniques will not be effective. They therefore

use the bootstrap to construct a lower bound for the un-confounded part of the noise variance and conclude that the assumed number of dimensions, $k$, is too small if the lower bound seems too large.

In this paper we analyze more direct approaches, namely, the classical variance decomposition technique, and choosing $k$ using selection criteria. Yao et al. (2005) proposed using a functional version of Akiake's information criterion to select $k$, justified via an appeal to a pseudo-Gaussian likelihood argument and the results of Shibata (1981). Here we consider criteria constructed using optimal encoding, description length principles. This conceptual framework, which is reviewed in Hansen and Yu (2001), see also Rissanen (2007) and Grünwald (2007), provides a well established rationale that is directly applicable to the current functional data setting. We show below that it leads to techniques that circumvent confounding issues, and we develop the theoretical properties of the techniques within a functional data framework.

The paper proceeds as follows. The next section considers aspects of the basic structure of functional data, and introduces two examples that are used to illustrate our ideas, the first taken from mass-spectroscopy and the second from climatology. As part of our analysis we provide, in Section 3, a flexible definition of the dimension of $X$ that depends on a signal-plus-noise decomposition derived from the function's Karhunen–Loève expansion. By couching the concept of dimensionality directly in terms of the actually observed process our definition obviates the need to explicitly posit the existence of separate signal and noise components, although data generating mechanisms that consist of a signal embedded in noise are encompassed as a special case and we show that our definition will coincide with the finite dimension of the signal in low noise settings. In Section 4 we develop some preliminary limit results under relatively weak regularity conditions. Section 5 discusses the classical variance decomposition technique. We show that the statistics computed using this technique converge to their population counterparts, but, nevertheless, the dimension chosen by this method will not be consistent in general. Section 6 examines two description length criteria for determining the dimension of functional data. We prove that the criteria behave in a coherent manner asymptotically and that in low noise settings they will produce consistent estimates of the true finite dimension of a signal that is embedded in noise. In Section 7 the data sets presented in Section 2 are used to illustrate the practical impact of the different methods considered. Section 8 examines the application and efficacy of different varieties of non-parametric and semi-parametric bootstrap, and using various versions of these demonstrates the workings of our theoretical results. The proofs are assembled in an Appendix.

# 2 Basic Data Structures

Although the function $X$ is defined on the interval $[0, \tau]$ it is seldom observed there, but is instead observed on a discrete subset of points. Here we will presume that each data curve $X_i(t)$ is observed on a grid of $T$ points $t_u$, $u = 1, \ldots, T$, with $0 \le t_1 < t_2 < \ldots < t_T \le \tau$. Thus the raw data in a set $\mathcal{X} = \{X_1, ..., X_n\}$ of $n$ observations on $X$ will consist of an $n \times T$ data matrix $\mathbb{X} = [X_{ru}]$ where, setting $\upsilon_j = \xi_j/\omega_j$ with $\omega_j = \sqrt{\lambda_j}$, we have

$$X_{ru} = \mu(t_u) + \sum_{j=1}^{\infty} \upsilon_{r,j}\, \omega_j\, \rho_j(t_u), \tag{3}$$

for $r = 1, \ldots, n$ and $u = 1, \ldots, T$.

Example 1: The graphs in Figure 1 present mass–chromatograms averaged across $n_1 = 100$ ovarian cancer patients, and $n_2 = 116$ healthy controls (including 16 individuals with benign tumors). The measurements were collected from a surface-enhanced

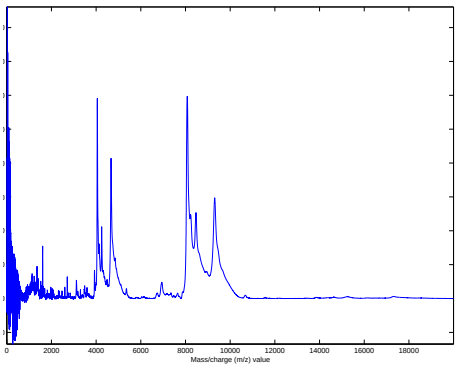


(a) Average proteomic spectrum of $n_1 = 100$ ovarian cancer patients.

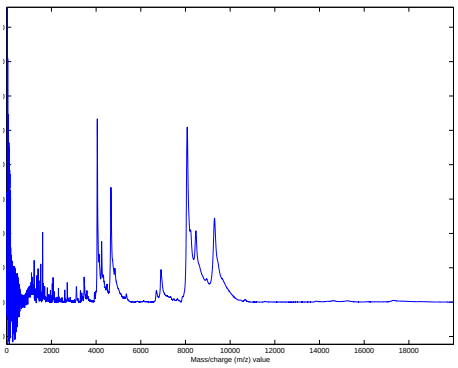


(b) Average proteomic spectrum of $n_2 = 116$ healthy controls.

Figure 1: Mass-chromatograms from ovarian cancer data.

laser desorption-ionization system (see Thiele, 2003; Banks, 2003). Each spectrum gives the relative amplitude measured at 15154 mass-charge ($\mu z$) values on the interval $[0, 18000]$. Thus we have an overall sample of $n_1 + n_2 = n = 216$ curves, where each curve is the proteomic spectrum of an individual patient observed on a grid of $T = 15154$ points. The ovarian cancer (OC) data was downloaded from `http://clinicalproteomics.steem.com`.

Despite being similar in appearance overall, the spectral profiles in Figures 1a and 1b exhibit different features, witness the peaks at about $4000\mu z$ and $7000\mu z$ for example. The question of scientific interest here is whether or not differences in individual mass-chromatograms can be reliably used to discriminate cancer patients from healthy controls and thereby construct a simple screening device.

Example 2: Figure 2 presents monthly observations on the Southern Oscillation Index (SOI) for the period 1900-2004 inclusive, graphed as a sequence of repeated measures on the annual cycles. The data, constructed by the Australian Meteorological Office, can be downloaded from `http://www.environment.gov.au`. Treating each year as a single observation on a random function representing the annual cycle gives us a

sample of $n = 105$ data points where each function is observed on a grid of $T = 12$ regularly spaced intervals.

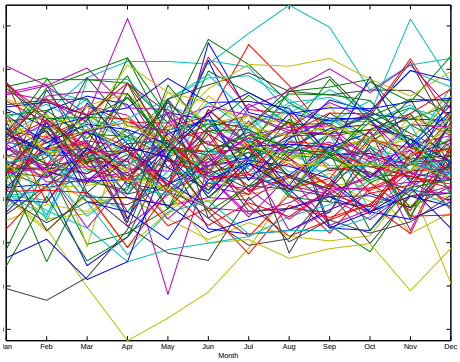


Figure 2: Annual repeated measures on Southern Oscillation Index: observed annual cycles in period 1900-2004.

No obvious patterns emerge from simple visual inspection of the observed annual cycles. The values appear to fluctuate more or less randomly around zero, although there is evidence of some extreme negative values in the summer and autumn months, and extreme positive values in the winter and spring months. Variations in the SOI are thought to be very influential in determining annual weather patterns in the southern hemisphere (el nino and el nina effects) and we would like to be able to determine if the apparently erratic behaviour seen in Figure 2 disguises more systematic patterns.

Let the observed mean of the data in $\mathbb{X}$ be $\bar{\mathbb{X}} = \mathbf{s}'\mathbb{X}/n$ where $\mathbf{s} = (1, \ldots, 1)'$ and set $\mathbf{C} = (1 - \mathbf{s}\mathbf{s}'/n)$, the centering matrix. Then the mean centered data matrix is given by $(\mathbb{X} - \mathbf{s}'\bar{\mathbb{X}}) = \mathbf{C}\mathbb{X} = \mathbf{X}$, say. A standard approach to estimating the covariance kernel is to take

$$\bar{\Gamma}(u, v) = \frac{1}{n}\sum_{i=1}^{n}\{X_i(u) - \bar{X}(u)\}\{X_i(v) - \bar{X}(v)\}$$

as an estimator of $\Gamma(u, v)$ where $\bar{X}(u) = n^{-1}\sum_{i=1}^{n} X_i(u)$. Setting $\mathbf{G} = (\mathbb{X} - \mathbf{s}\bar{\mathbb{X}})'(\mathbb{X} - \mathbf{s}\bar{\mathbb{X}})/n = (\mathbf{X}'\mathbf{X})/n$ we have $\mathbf{G} = [\bar{\Gamma}(t_u, t_v)]$ for $u, v = 1, \ldots, T$.

Now let the singular value decomposition of $\mathbf{X}$ be denoted by

$$\mathbf{X} = n^{1/2}\mathbf{U}\mathbf{L}\mathbf{R}' \tag{4}$$

where $\mathbf{U}'\mathbf{U} = \mathbf{R}'\mathbf{R} = \mathbf{I}_m$, $m = rank(\mathbf{X}) = \min\{n, T\}$, and the diagonal matrix $\mathbf{L} = \mathrm{diag}(\sqrt{l_1}, \sqrt{l_2}, \ldots, \sqrt{l_m})$ where $l_1, \ldots, l_m$ lists the positive eigenvalues of $\mathbf{G}$ in descending order. The columns $\mathbf{u}_{\cdot 1}, \ldots, \mathbf{u}_{\cdot m}$ of $\mathbf{U}$ are the normalized eigenvectors of $\mathbf{X}\mathbf{X}'/n$ and the columns $\mathbf{r}_{\cdot 1}, \ldots, \mathbf{r}_{\cdot m}$ of $\mathbf{R}$ are the normalized eigenvectors of $\mathbf{G}$. The expansion in (4) provides an empirical counterpart to the Karhunen–Loève expansion in (3) in that a random curve in $\mathbb{X}$ can be written as

$$X_i(t_u) = \bar{X}(t_u) + \sqrt{n}\sum_{j=1}^{m} u_{ij}\, w_j\, r_j(t_u)\,, \tag{5}$$

where $w_j = \sqrt{\tau l_j/T}$ and $(\sqrt{\tau/T})r_j(t_u) = r_{uj}$, the $u$'th element of $\mathbf{r}_{\cdot j} = (r_{1j}, \ldots, r_{Tj})'$. In addition we have $\bar{\Gamma}(t_u, t_v) = (\tau/T)\sum_{j=1}^{m} l_j r_j(t_u) r_j(t_v)$, which in turn mimics the

spectral decomposition of the covariance in (2). The pairs $(\tau l_j/T, r_j(t_u))$, which are of course the basic statistics of functional principle component analysis (Ramsay and Silverman, 1997; Ferraty and Vieu, 2006), will be used to estimate the eigenvalue, eigenfunction pairs $(\lambda_j, \rho_j(t_u))$, $j = 1, \ldots, m$, and will form the fundamental building blocks of our subsequent practical methodology.

# 3 Signal, Noise and Dimension

## 3.1 Signal–plus–Noise Representations

Suppose that the Karhunen–Loève expansion of $X$ is truncated after $k$ terms. Then the finite expansion $S_k(t) = \mu(t) + \sum_{j=1}^{k} \xi_j \rho_j(t)$ can be used to approximate the function $X$. We can think of this as the signal component and the remainder, $N_k(t) = \sum_{j=k+1}^{\infty} \xi_j \rho_j(t)$, can be thought of as noise. Thus,

$$X(t) = S_k(t) + N_k(t) \tag{6}$$

yields an orthogonal decomposition of $X$ in $\mathcal{L}^2_{[0,\tau]}$ that is optimal for a given $k$, in the sense that $S_k(t)$ provides the minimum mean squared error approximation to $X$. Moreover, $N_k(t)$ converges to zero as $k$ increases. The decomposition in (6) holds true for all $k \in \mathbb{N} = \{1, 2, 3, \ldots\}$, however, and it follows that this decomposition cannot be used by and of itself to define the dimensionality of the process.

A possible solution to this problem is to proceed constructively and to suppose, following Hall and Vial (2006), that the observations are made up of realizations on an actual process of interest, $Y(t)$, that is in truth finite dimensional, to which a zero mean noise process, $\delta Z(t)$, representing experimental error, measurement error and so on, has been added. Thus

$$X(t) = Y(t) + \delta Z(t) \tag{7}$$

where $Y(t) = \mu(t) + \sum_{j=1}^{\kappa} \nu_j \varphi_j(t)$, $Z(t) = \sum_{j=1}^{\infty} \zeta_j \psi_j(t)$, and $\delta$ is a positive constant. The difficulty here is that (7) is observationally equivalent to

$$\begin{aligned} X(t) &= \mu(t) + \sum_{j=1}^{\kappa} (\nu_j + \delta \sum_{i=1}^{\infty} \zeta_i \beta_{ij}) \varphi_j(t) + \delta \sum_{j=\kappa+1}^{\infty} (\sum_{i=1}^{\infty} \zeta_i \beta_{ij})\, \varphi_j(t) \\ &= Y'(t) + \delta Z'(t) \quad \text{say}\,, \end{aligned} \tag{8}$$

where the sequence $\varphi_1(t), \varphi_2(t), \ldots, \varphi_\kappa(t), \ldots$ is a complete orthonormal extension of $\varphi_j(t)$, $j = 1, \ldots, \kappa$, and $\beta_{ij} =< \psi_i, \varphi_j >$ for $i, j = 1, 2, \ldots$, (see Hall and Vial, 2006, Sections 2.1 & 2.2). It can be seen from (8) that the lower dimensional components of the noise $\delta Z(t)$ are confounded with those of the signal $Y(t)$, and that $Y'(t)$ and $\delta Z'(t)$ are orthogonal, so the original noise or error component cannot be identified.

In their analysis Hall and Vial (2006) argue for a consideration of the low noise case, wherein the scale parameter $\delta \to 0$, on didactic grounds. They show that in the low noise case $\delta^2 \sum_{j=\kappa+1}^{\infty} E[\zeta_j^2]$ – "the greatest knowable lower bound to all possible values of noise variance" – is identifiable and they use this as the bench-mark for assessing noise levels. In empirical situations, however, the amount of noise need not be small and the representations in (7) and (8) are equivalent for all values of $\delta$. Indeed,

adopting a parallel development to that leading to (8), we also have

$$\begin{aligned} X(t) &= \mu(t) + \sum_{j=1}^{\kappa} c_j\,\psi_j(t) + \sum_{j=\kappa+1}^{\infty} c_j\,\psi_j(t) \\ &= S'_\kappa(t) + N'_\kappa(t)\,, \end{aligned} \tag{9}$$

wherein $c_j = \sum_{l=1}^{\kappa} \nu_l < \varphi_l, \psi_j > + \delta\zeta_j$ for $j = 1, 2, \ldots$. In (9) the signal $Y(t)$ has been confounded with the noise $\delta Z(t)$ and the resulting decomposition is clearly observationally equivalent to (6) with $k = \kappa$. For moderate to large values of $\delta$ the question of what constitutes the dimension of the realized process $X$ therefore remains moot.

## 3.2 The Signal-to-Noise Ratio and Dimension

Expression (2) gives the spectral decomposition of $\Gamma(t,s)$, and the equality $\int_0^\tau \Gamma(t,t)dt = \sum_{j=1}^{\infty} \lambda_j$ is interpreted statistically as indicating the contribution of each term in (1) to the overall variance of $X$ in $[0,\tau]$. If we set

$$\pi_k = \frac{\sum_{j=1}^{k} \lambda_j}{\sum_{j=1}^{\infty} \lambda_j}\,, \tag{10}$$

then $SNR(k) = \pi_k/(1-\pi_k)$ is the natural measure of the signal-to-noise ratio of the decomposition in (6). Given $\alpha$, where $0 \le \alpha < 1$, let $SNR_\alpha = \{k \in \mathbb{N} : SNR(k) \ge \alpha/(1-\alpha)\}$.

**Definition 1** *Let $k_\alpha \in SNR_\alpha$ be such that $k \ge k_\alpha$ for all $k \in SNR_\alpha$. Then $X$ will be said to be a process of dimension $k_\alpha$ at signal-to-noise ratio (SNR) level $\alpha/(1-\alpha)$.*

Note that the designated dimension of $X$ is the smallest value of $k$ such that $SNR$ equals or exceeds the specified lower bound.

Clearly, $k_\alpha$ will depend on both the assigned level of resolution, as determined by $\alpha$, and the structure of $X$. For the process in (7), for example, $SNR(k)$ can exceed $\alpha/(1-\alpha)$ for $k < \kappa$ if $\alpha$ is small, but need not do so if $\alpha$ is large. As $\delta \to 0$, however, $SNR(k)$ will exceed any value $\alpha/(1-\alpha) < \infty$ for all $k \ge \kappa$, and $X$ will be deemed to be a process of dimension $\kappa$ at $SNR$ level $\alpha/(1-\alpha)$ for all $\alpha > \pi_{\kappa-1}$. To verify this let $\eta_j$, $j = 1, \ldots, \kappa$ and $\theta_j$, $j = 1, 2, \ldots$, equal the eigenvalues of $\Gamma_Y(t,s) = Cov[Y(t), Y(s)]$ and $\Gamma_Z(t,s) = Cov[Z(t), Z(s)]$, respectively. Clearly $X(t)$ converges to $Y(t)$ in $\mathcal{L}^2_{[0,\tau]}$ as $\delta \to 0$ and since $Y(t)$ lies in the space spanned by $\varphi_j(1), \ldots, \varphi_j(\kappa)$,

$$\begin{aligned} \lambda_j &= \int_0^\tau \int_0^\tau \rho_j(t)\Gamma(t,s)\rho_j(s)dtds \\ &= \int_0^\tau \int_0^\tau \varphi_j(t)(\Gamma_Y(t,s) + \delta^2\Gamma_Z(t,s))\varphi_j(s)dtds + R_{\delta,j} \\ &= \begin{cases} \eta_j + \delta^2 \sum_{i=1}^{\infty} \theta_i \beta_{ij}^2 + R_{\delta,j}, & j \le \kappa; \\ \delta^2 \sum_{i=1}^{\infty} \theta_i \beta_{ij}^2 + R_{\delta,j}, & j > \kappa. \end{cases} \end{aligned} \tag{11}$$

where $R_{\delta,j} = \int_0^\tau \int_0^\tau \Gamma(t,s)(\rho_j(t)\rho_j(s) - \varphi_j(t)\varphi_j(s))dtds$. Now

$$\begin{aligned} |R_{\delta,j}| &\le \left\{ \lambda_j + \left( \int_0^\tau \left[ \int_0^\tau \varphi_j(t)\Gamma(t,s)dt \right]^2 ds \right)^{1/2} \right\} \|\rho_j - \varphi_j\| \\ &\le \left\{ \lambda_j + \eta_j + 2\delta^2 \sum_{i=1}^{\infty} \theta_i \right\} \|\rho_j - \varphi_j\| \end{aligned}$$

and it can be shown, see the approximation lemmas in Hall et al. (2006, Lemma 1 & 2, p.1508), that $\|\rho_j - \varphi_j\|^2 = O(\delta^4)$. Note in addition that $\sum_{j=1}^{\infty} R_{\delta,j}$ is identically zero because $\sum_{j=1}^{\infty} \int_0^\tau \int_0^\tau \Gamma(t,s)\varphi_j(t)\varphi_j(s)dtds$ equals $\sum_{j=1}^{\infty} \int_0^\tau \int_0^\tau \Gamma(t,s)\rho_j(t)\rho_j(s)dtds = \sum_{j=1}^{\infty} \lambda_j$, the trace of the covariance kernel. Thus we find that

$$SNR(k) = \frac{\pi_k}{1-\pi_k} = \frac{\sum_{j=1}^{\kappa} \eta_j + O(\delta^2)}{O(\delta^2)}$$

for any $k \geq \kappa$ and hence $SNR(k)$ will exceed $\alpha/(1-\alpha)$ for any $\alpha \geq \pi_{\kappa-1}$ as $\delta \to 0$.

# 4 Some Preliminary Results

Because we do not want to explicitly postulate the existence of separate signal and noise processes our basic assumptions are presented in terms the observed process itself.

**Assumption 1** *The observed process $X \in \mathcal{L}^2_{[0,\tau]}$, has a Karhunen–Loève expansion as in* (1)*, and covariance kernel $\Gamma(t,s)$ with spectral decomposition as in* (2)*, where the eigenvalues $\lambda_j > 0$, $j = 1, \ldots$ are distinct.*

Assumption 1 recognizes that functional data observed in practice is inherently infinite dimensional. It is, in some ways, the functional analog of the Wold representation employed in classical time series analysis.

**Assumption 2** *Let $\mathcal{X} = \{X_1, ..., X_n\}$ denote a sample of $n$ observations on a process $X$ where each curve is observed on a grid of $T$ points $t_u$ with $0 \leq t_1 < t_2 < \ldots < t_T \leq \tau$. Then for all $s = 1, \ldots, n$*

$$E[X_s(t_u)] = \mu(t_u) \tag{12}$$

*and*

$$E[\{X_s(t_u) - \mu(t_u)\}\{X_s(t_v) - \mu(t_v)\}] = \Gamma(t_u, t_v)\,. \tag{13}$$

*Furthermore, for all $u = 1, \ldots, T$,*

$$\sup_s \sum_{r=0}^{\infty} Cov[X_s(t_u)X_{s+r}(t_u)] < C_1 < \infty\,, \tag{14}$$

*and setting $\Xi_s(uv) = \{X_s(t_u) - \mu(t_u)\}\{X_s(t_v) - \mu(t_v)\}$, then for all $u, v = 1, \ldots, T$,*

$$\sup_s \sum_{r=0}^{\infty} Cov[\Xi_s(uv)\Xi_{s+r}(uv)] < C_2 < \infty\,. \tag{15}$$

The first part of Assumption 2 amounts to supposing that the observations behave like the realization of a weakly stationary functional process with a common mean function and covariance kernel. The second part places bounds on the auto-covariance of function values observed at different points along the abscissa, and provides sufficient conditions to ensure that $\bar{\mathbb{X}}$ and $\mathbf{G}$, the sample mean and covariance, will converge to their population counterparts $\boldsymbol{\mu} = (\mu(t_1), \ldots, \mu(t_T))$ and $\boldsymbol{\Gamma} = [\Gamma(t_u, t_v)]$, $u, v = 1, \ldots, T$, respectively.

**Lemma 1** *Let* $\mathbf{d} = \bar{\mathbb{X}} - \boldsymbol{\mu}$ *and set* $\mathbf{D} = [D_{kl}]$ *where*

$$D_{kl} = \frac{1}{n}\sum_{s=1}^{n}\{X_s(t_u) - \mu(t_u)\}\{X_s(t_v) - \mu(t_v)\}] - \Gamma(t_u, t_v) \quad u, v = 1, \ldots, T\,.$$

*Then under Assumptions 1 and 2 the inequalities* $E[\|\mathbf{d}\|^2] < 2C_1T/n$ *and* $E[\|\mathbf{D}\|^2] < 2C_2T^2/n$ *obtain for all* $T$*.*

It follows directly from Lemma 1, via Markov's inequality, that $\|\mathbf{d}\|^2 = o_p(T/n^{1-\beta})$ and $\|\mathbf{D}\|^2 = o_p(T^2/n^{1-\beta})$ for any $\beta$, $0 < \beta \leq 1$. From the expression $\mathbf{G} - \boldsymbol{\Gamma} = \mathbf{D} - \mathbf{d}'\mathbf{d}$ we can also deduce that $\|\mathbf{G} - \boldsymbol{\Gamma}\|^2 \leq (\|\mathbf{D}\| + \|\mathbf{d}\|^2)^2$, and hence we can conclude that $\|\mathbf{G} - \boldsymbol{\Gamma}\|^2 = o_p(T^2/n^{1-\beta})$ and $\mathrm{plim}(\|T^{-1}(\mathbf{G} - \boldsymbol{\Gamma})\|^2) = 0$. These properties lead us to the following result.

**Lemma 2** *Suppose that Assumptions 1 and 2 hold. Then for any* $\beta \in (0, 1]$

$$\sum_{j=1}^{m}(l_j - \ell_j)^2 = o_p(T^2/n^{1-\beta}) \tag{16}$$

*as* $n \to \infty$ *where* $\ell_j$*,* $j = 1, \ldots, T$*, denote the eigenvalues of* $\boldsymbol{\Gamma}$*. Moreover, if* $T \to \infty$ *then*

$$\max_{1\leq j\leq m}\left|\frac{l_j}{T} - \frac{\lambda_j}{\tau}\right| = o_p(1/n^{(1-\beta)/2}) + o(1) \tag{17}$$

*and*

$$\left|\sum_{j=1}^{m}\frac{l_j}{T} - \sum_{j=1}^{\infty}\frac{\lambda_j}{\tau}\right| = o_p(m/n^{(1-\beta)/2}) + o(m)\,. \tag{18}$$

Interestingly enough, although our assumptions are sufficiently general to apply to time series type data, as in Example 2, the convergence rate for the eigenvalues of $o_p(n^{-(1-\beta)/2})$ given in Lemma 2 compares favourably with the $O_p(n^{-1/2})$ rate obtained by Hall and Hosseini-Nasab (2006) under simple random sampling.

# 5 Variance decomposition

A commonly employed, classical approach to determining the number of sample principle components to retain in a description of an observed variance-covariance matrix is that based upon an examination of the proportion of variance explained. Thus, suppose that we are interested in accounting for $\alpha 100\%$ of the total variation in $\mathbb{X}$ where $0 < \alpha \leq 1$. Then the variance decomposition method selects $\hat{k}_\alpha$ principle components where $\hat{k}_\alpha$ is the smallest value of $k$ such that

$$\widehat{\pi}_k = \frac{\sum_{j=1}^{k} l_j}{\sum_{j=1}^{m} l_j} \tag{19}$$

equals or exceeds $\alpha$. For the null model $\widehat{\pi}_0 \equiv 0$ and for the saturated model $\widehat{\pi}_m = 1$. For a detailed description of this and other methods see Jolliffe (2002, Chapter 6).

This approach is frequently adopted in the analysis of functional data (see, *inter alia*, Chiou and Li, 2007, Section 2.2.1) and in practice the value of $\hat{k}_\alpha$ is often chosen by reference to a graph of $\widehat{\pi}_k$ against $k$, similar to a 'scree plot'. Such a graph is monotonically non-decreasing in $k$ with $\widehat{\pi}_k < \alpha$ for $k < \hat{k}_\alpha$ and $\widehat{\pi}_k \geq \alpha$ for $k \geq \hat{k}_\alpha$,

and a popular rule-of-thumb is to look for the value of $k$ that accounts for at least $75-80\%$ of the total variation.

Noting that $\pi_k$ equals the proportion of variation in $X$ attributable to the signal $S_k(t)$, and that $1-\pi_k$ equals that associated with the noise $N_k(t)$, we can see that the variance decomposition method is closely aligned with Definition 1. In particular, $\widehat{\pi}_k$ can obviously serve as an estimator of $\pi_k$.

**Lemma 3** *Let $\pi_k$ be defined as in* (10) *and $\widehat{\pi}_k$ as in* (19)*, and suppose that Assumptions 1 and 2 hold. Then* $\max_{1\leq k\leq m}|\widehat{\pi}_k-\pi_k| = o_p(1/n^{(1-\beta)/2})+o(1)$.

Similarly, the ratio $\widehat{SNR}(k)=\widehat{\pi}_k/(1-\widehat{\pi}_k)$ is the empirical counterpart to $SNR(k)$, and the above rule-of-thumb amounts to selecting $k$ so as to obtain an observed signal-to-noise ratio $\widehat{SNR}(k)\geq\alpha/(1-\alpha)$ with the value of $\alpha$ *pre-assigned* by the practitioner to a value in excess of 0.75.

**Theorem 1** *Assume that the conditions of Lemma 3 hold. Then $\widehat{SNR}(k)$ converges in probability to $SNR(k)$ for $k=1,\ldots,m$ as $(n,T)\to(\infty,\infty)$. Furthermore, if $X$ is a process of dimension $k_\alpha$ at SNR level $\alpha/(1-\alpha)$ then $|\hat{k}_\alpha-k_\alpha|=o_p(1)$.*

Theorem 1 indicates that the variance decomposition method behaves in a coherent way, in that the underlying statistics converge to their population counterparts. Implementing this technique as a means of selecting a dimension suitable for practical application requires the user to specify a value for $\alpha$, however, and such a choice is *ad hoc*. Consider the signal-plus-noise process in (7). If $k<\kappa$ then, by Theorem 1,

$$\begin{aligned}\widehat{SNR}(k) &= \frac{\pi_k}{1-\pi_k}+o_p(1/n^{(1-\beta)/2})+o(1)\\ &= \frac{\sum_{j=1}^{k}\eta_j+O(\delta^2)}{\sum_{j=k+1}^{\kappa}\eta_j+O(\delta^2)}+o_p(1/n^{(1-\beta)/2})+o(1)\,.\end{aligned}$$

Hence $\widehat{SNR}(k)$ converges to a value that will exceed $\alpha/(1-\alpha)$ if $\alpha<\pi_k$, but will remain bounded as $\delta\to 0$. It follows that $\mathrm{plim}(\hat{k}_\alpha)=k_\alpha<\kappa$ for any $\alpha\leq\pi_{\kappa-1}$. This indicates that the variance decomposition method is not consistent for the true dimension of $X$ in the conventional sense. We might attempt to retrieve the situation by setting $\alpha=\alpha(n)$ where $\alpha(n)\to 1$ as $n\to\infty$, but our current results provide no guide to a suitable choice.

# 6 Description Length

Optimal encoding, description length principles lead to data generated rules for selecting $k$ that will produce a finite dimensional representation of $X$ that is as close an approximation as is possible, and uses the smallest number of parameters necessary, whilst adequately representing the structure and information contained in the data. Competing specifications are compared on the basis of their complexity, which is measured by reference to a criterion function. In the notation of this paper, one such criterion function is

$$CL_2(k)=\frac{n}{2}\log\left(V(k)\right)+\frac{k}{2}\log\left(n\right)\,, \tag{20}$$

where the residual mean square

$$V(k) = \frac{1}{nT}\sum_{i=1}^{n}\sum_{u=1}^{T}(X_i(t_u) - \bar{X}(t_u) - \sqrt{n}\sum_{j=1}^{k} u_{ij}\, w_j\, r_j(t_u))^2 \,. \tag{21}$$

The function $CL_2(k)$ may be viewed as a two stage coding scheme, or code length, in which the first part represents the cost of the data compression and the second measures the code length used to encode the data when using $k$ basis functions. The criterion $CL_2(k)$ achieves the stated goals since: (i) $TV(k) = \|\mathbf{G} - \widehat{\mathbf{G}}_k\|^2$ where $\widehat{\mathbf{G}}_k = \sum_{j=1}^{k} l_j \mathbf{r}_{\cdot j}\mathbf{r}'_{\cdot j}$ and if $\overline{\mathbf{G}}_k$ is a matrix of rank $k$ used to approximate $\mathbf{G}$, then $\|\mathbf{G} - \overline{\mathbf{G}}_k\|^2$ is minimized at $\overline{\mathbf{G}}_k = \widehat{\mathbf{G}}_k$; and (ii) $CL_2(k)$ will exhibit a preference for smaller values of $k$, other things being equal.

To relate $CL_2(k)$ to the Karhunen–Loève decomposition of $X$, we can expand (21) and substitute into (20) to give $CL_2(k) = nDL_2(k)/2 + C_n$ where

$$DL_2(k) = \log(1 - \widehat{\pi}_k) + k\frac{\log(n)}{n} \tag{22}$$

and the 'constant' $C_n = \log\left(\frac{1}{nT}\sum_{i=1}^{n}\sum_{u=1}^{T}(X_i(t_u) - \bar{X}(t_u))^2\right)$ is independent of $k$. We may think of $DL_2(k)$ as giving the description length per data point. The selected dimension, the minimum description length, is given by $\widetilde{k}_2 = \arg\min_{0\le k<m} DL_2(k)$ .

Description length criteria are not unique and an alternative criterion proposed by Rissanen (2000) for signal denoising is the, so called, normalized minimum description length. In the current context this criterion gives rise to a consideration of

$$\begin{aligned} DL_N(k) =& \log(1 - \widehat{\pi}_k) + \frac{k}{n}\log\left(\frac{\widehat{\pi}_k}{1 - \widehat{\pi}_k}\left\{\frac{nT - \nu(k)}{\nu(k)}\right\}\right) \\ &+ \frac{1}{n}\log\left(\nu(k)(nT - \nu(k))\right) \,, \end{aligned} \tag{23}$$

wherein $\nu(k) = k(m+1) - \frac{1}{2}k(k+1)$ denotes the degrees of freedom in the $k$th singular value representation of the $nT$ effective observations in $\mathbf{X}$. As above, the associated minimum description length, $\widetilde{k}_N$, is given by the value of $k \in \{0, \ldots, m-1\}$ that minimizes $DL_N(k)$. For a discussion of other encoding, description length schemes, see Hansen and Yu (2001) and Grünwald (2007).

Members of the statistics fraternity will recognize $CL_2(k)$ as BIC, after Schwarz (1978). Schwarz criterion is well known to produce consistent order selection under appropriate assumptions and this raises the question of how, in the guise of $DL_2(k)$, it will behave under the current scenario. We therefore seek to characterize the properties of $DL_2(k)$, and $DL_N(k)$, when in truth $X$ does not admit an exact finite expansion.

Towards this end, let us suppose that an oracle has told us the values of $\lambda_j$ $j = 1, 2, \ldots$. Set $\overline{DL}_2(k) = \log(1 - \pi_k) + k\log(n)/n$ and let $\overline{k}_2$ denote the value of $k \in \{0, \ldots, m-1\}$ that minimizes $\overline{DL}_2(k)$. Similarly, let $\overline{DL}_N(k)$ denote the value obtained by replacing $\widehat{\pi}_k$ by $\pi_k$ in $DL_N(k)$ and set $\overline{k}_N = \arg\min_{0\le k<m}\overline{DL}_N(k)$. Then for $a \in \{2, N\}$, the oracle will proclaim $X$ to be a process of dimension $\overline{k}_a$ at $SNR$ level $\alpha/(1-\alpha)$ where $\alpha = \pi_{\overline{k}_a}$.

**Theorem 2** *Suppose that Assumptions 1 and 2 hold. Then for both $a \in \{2, N\}$ we have $\left|\overline{DL}_a(k) - DL_a(k)\right| = o_p(1/n^{(1-\beta)/2}) + o(1)$ as $(n, T) \to \infty$. Furthermore,* $\lim_{(n,T)\to(\infty,\infty)} Prob[\widetilde{k}_a = \overline{k}_a] = 1$ .

Theorem 2 indicates that for large values of $n$ and $T$ both $DL_2(k)$ and $DL_N(k)$ are likely to be close to the values that would be obtained by the oracle. In particular, a corollary of Theorems 1 and 2 is that for both $a \in \{2, N\}$ $\text{plim}|\widehat{SNR}(\widetilde{k}_a) - SNR(\overline{k}_a)| = 0$. Thus the criterion functions behave in a coherent manner and for $(n, T)$ sufficiently large the practitioner will know the dimension of $X$ that the oracle would have proclaimed and the value of $SNR$ at which that proclamation would have been made.

We have already seen that the signal-plus-noise process $X$ in (7) has dimension $\kappa$ at $SNR$ level $\alpha/(1-\alpha)$ for all $\alpha > \pi_{\kappa-1}$ as $\delta \to 0$. In order to relate this to the values of $k$ selected by the description length criteria let us introduce an additional assumption.

**Assumption 3** *There exits constants $C$, $0 < C < \infty$, and $d$, $0 < d < 2$, such that $\inf_i \beta_{ij}^2 \geq Cg^j$, for all $j = 1, \ldots,$ where $g^2 = 1 - \delta^{2-d}$.*

The generalized Fourier coefficients $\beta_{ij}$ lie in the unit interval $[0, 1]$ because $\sum_{j=1}^{\infty} \beta_{ij}^2 = 1$ and Assumption 3 bounds the coefficients away from zero. This ensures that the contribution of the noise to the overall variation of $X$ on $[0, \tau]$ cannot be null, and that the components of $Z(t)$ that are orthogonal to $Y(t)$ cannot be identically zero.

**Theorem 3** *Suppose that $X(t) = Y(t) + \delta Z(t)$, as in (7). Suppose also that $Y(t)$ and $Z(s)$ are uncorrelated for all $t$ and $s$, and that Assumptions 1 and 2 hold. Then the probability that the event $\widetilde{k}_a \geq \kappa$ obtains converges to 1 as $(n, T) \to \infty$ for both $a \in \{2, N\}$. Furthermore, if Assumption 3 holds and $\delta \to 0$ such that $\delta^{2-d} nT/(n+T) \to 0$, then $\lim_{(n,T)\to(\infty,\infty)} Prob[|\widetilde{k}_a - \kappa| > \delta] = 0$ and $X$ will be deemed to be a process of dimension $\kappa$ at level $SNR_\alpha$ for all $\alpha > \pi_{\kappa-1}$.*

# 7 Illustrations

The asymptotic results presented above require that $(n, T) \to (\infty, \infty)$, but they do not impose any further restrictions on the orders of magnitude of $n$ and $T$. Thus they can be thought of as being applicable to both of the examples presented previously even though the relative sizes of $n$ and $T$ in the two cases are very different.

Example 1: Figure 3 graphs the values of $DL_2(k)$ and $DL_N(k)$ for $k$ in the range $0 \leq k < m$ when computed from the OC data. The figure clearly illustrates that

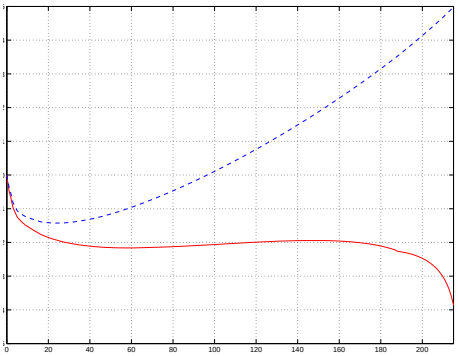


Figure 3: Graph of criterion $DL_N(k)$ (dotted line) and $DL_2(k)$ (solid line) when computed from the OC data.

the components of $DL_N(k)$ can counter-balance each other in such a way that the criterion has a well defined minimum at a relatively small value of $k$. Thus we find that $\widetilde{k}_N = 25$.

The behaviour of $DL_2(k)$ merits elaboration. Starting at the origin, as $k$ increases $DL_2(k)$ exhibits two turning points, a local minimum at $k = 57$ and a local maximum at $k = 147$, before finally reaching a global minimum at the saturation boundary. Thus, as $k \to m$ and $\widehat{\pi}_k \to 1$ the increase in $k \log(n)/n$ is no longer large enough to counteract the decrease in $\log(1-\widehat{\pi}_k)$. This presents a problem if we continue to search for the global minimum since $\widehat{\pi}_k \geq 0.995$ for $k \geq 135$, suggesting that any variation due to bases with an index greater than 135 is very small and should be attributed to the noise rather than the signal component. In this case, a straightforward solution is available. We could either (i) restrict the search to $k \in \{0, \ldots, \hat{k}_\alpha\}$ for some $\alpha \geq 0.99$, say, or (ii) search for the first local minimum, starting from the null model. Both approaches result in the criterion selecting $\widetilde{k}_2 = 57$.

We also evaluated $\hat{k}_\alpha$ using values of $\alpha$ that bound those recommended in Chiou and Li (2007, Section 2.2.1), namely $\hat{k}_{0.75} = 6$ and $\hat{k}_{0.99} = 103$. These values clearly indicate the sensitivity of $\hat{k}_\alpha$ to the assigned level of resolution. A range of 98 possible values for $k$ is too broad to be of any help in deciding what dimension to actually use in practice, but $\hat{k}_{0.75}$ and $\hat{k}_{0.99}$ do provide a useful point of comparison for illustrative purposes.

The selected dimensions are reproduced in Table 1, together with their associated estimates $\widehat{\pi}_k$ and $\widehat{SNR}(k)$. Table 2 presents the results obtained when the different

Table 1: Selected dimensions for OC Data.

| Criterion | $k$ | $\widehat{\pi}_k$ | $\widehat{SNR}(k)$ |
|---|---|---|---|
| $\hat{k}_{0.75}$ | 6 | 0.7697 | 3.3424 |
| $\hat{k}_{0.99}$ | 103 | 0.9901 | 100.0672 |
| $\widetilde{k}_2$ | 57 | 0.9722 | 34.9152 |
| $\widetilde{k}_N$ | 25 | 0.9235 | 12.0746 |

dimensions are used in conjunction with the non-parametric functional classification procedure introduced in Hall et al. (2001) to discriminate cancer patients from healthy controls (*c.f.* Ferraty and Vieu (2003) and Chiou and Li (2007)). The overall error rate,

Table 2: Classification Results for OC Data.

| Criterion | $k$ | Overall error% | Sensitivity% | Specificity% |
|---|---|---|---|---|
| $\hat{k}_{0.75}$ | 6 | 19.44% | 83% | 74.85% |
| $\hat{k}_{0.99}$ | 103 | 14.81% | 73% | 95.69% |
| $\widetilde{k}_2$ | 57 | 10.65% | 83% | 94.83% |
| $\widetilde{k}_N$ | 25 | 14.81% | 79% | 90.52% |

and the sensitivity and specificity, were calculated using jackknife cross-validation. Since the selection criteria are not geared towards minimizing classification errors, the relative merits of the different values of $k$ seen in Table 1 are not directly mirrored in the measures given in Table 2. Nevertheless, it is apparent that even functional data that is observed on a grid of several thousands of points can be reduced to as few as fifty, or even twenty, or so dimensions whilst maintaining very creditable performance.

Example 2: Upon examination of $\widehat{\pi}_k$ for the SOI data we find that the first four basis functions account for 79.61% of the observed annual variation, suggesting that the variance decomposition method used in conjunction with the commonly employed rule-of-thumb would select $k = 4$. The first four basis functions are graphed in Figure 4. Although it is not difficult to imagine different combinations of these basis functions

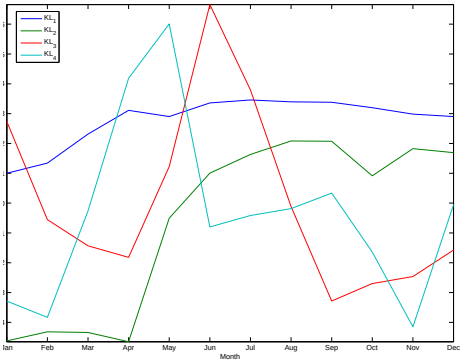


Figure 4: Dominant basis functions for SOI data.

giving rise to the different curves seen in Figure 2, from Figure 5, which graphs the values of $DL_2(k)$ and $DL_N(k)$ for $k$ in the range $0 \leq k < m$, we can see that both

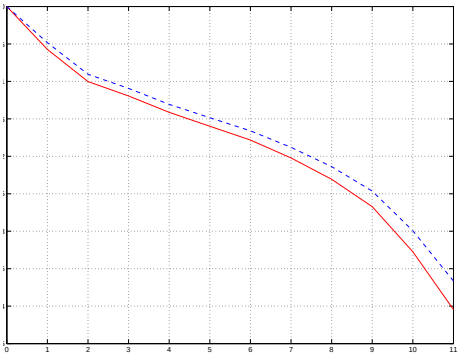


Figure 5: Graphs of $DL_2(k)$ and $DL_N(k)$ when computed from the SOI data.

criteria will select the most profligate model available, and searching for the first local minimum still leads to the selection of the saturated model.

These outcomes suggest that the behaviour of SOI observed in Figure 2 cannot be attributed to variation about more dominant, common annual cycles. Rather, the oscillations and extremes are due to aberrant values of the SOI being generated throughout particular years, suggesting that predicting the so called "g-phases", as discussed in Stone et al. (2000), could be a useful tool in forecasting future el nino/el nina effects and their associated weather patterns.

# 8 The Bootstrap

Given the raw data $\mathcal{X} = \{X_1, ..., X_n\}$ of $n$ observations on $X$, an obvious way to get some idea of the sampling variability of a statistic of interest is to re-sample from $\mathcal{X}$

and construct a bootstrap replication $\mathcal{X}^* = \{X_1^*, ..., X_n^*\}$. By repeatedly generating different bootstrap replications an approximation to the statistic's distribution can be constructed. This is precisely the technique employed in Hall and Vial (2006). Here we wish to investigate the application and efficacy of different forms of the bootstrap.

First, note that the bootstrap replications are obtained by re-sampling from the rows of

$$\mathbb{X} = \mathbf{s}\bar{\mathbb{X}} + n^{1/2}\mathbf{ULR}', \tag{24}$$

wherein the right hand side is the matrix-vector equivalent of (5). Writing $\mathbb{X}^*$ for a bootstrap data matrix we have

$$\mathbb{X}^* = \mathbf{S}\mathbb{X} = \mathbf{Ss}\bar{\mathbb{X}} + n^{1/2}\mathbf{SULR}' = \mathbf{s}\bar{\mathbb{X}} + n^{1/2}\mathbf{U}^*\mathbf{LR}', \quad \text{say}, \tag{25}$$

where $\mathbf{S}$ represents a randomly chosen $n \times n$ selection matrix. From (25) we can see that the bootstrap replications of the process can be generated in the following manner: Bootstrap Step

B1. Hold the mean $\bar{X}(t_u)$, the eigenvalues $l_j$, $j = 1, \ldots, m$, and the basis functions $r_j(t_u)$, $j = 1, \ldots, m$, fixed at their realized values;

B2. For $i = 1, \ldots, n$ generate bootstrap replications $u_{ij}^*, j = 1, \ldots, m$, by taking independent and identically distributed (i.i.d.) random draws from $u_{ij}, j = 1, \ldots, m$;

B3. Construct the bootstrap sample $\mathcal{X}^* = \{X_1^*, ..., X_n^*\}$ where, for $i = 1, \ldots, n$, the bootstrap realization $X_i(t_u)^*$, $u = 1, \ldots, T$, is constructed as in (5) by replacing $u_{ij}, j = 1, \ldots, m$ by $u_{ij}^*, j = 1, \ldots, m$.

By Lemma 1 $\bar{X}(t_u)$ is a consistent estimate of $\mu$ and by Lemma 2 the $l_j/T$ provide consistent estimates of $\lambda_j/\tau$. From the following lemma we also know that the $r_j(t)$ estimate the basis functions $\rho_j(t)$ consistently.

**Lemma 4** *Assume that Assumptions 1 and 2 hold and that* $(n, T) \to (\infty, \infty)$. *Let* $r_j(t)$ *be interpolating cubic smoothing splines that pass through the knots* $(t_u, \sqrt{T}r_{uj}/\sqrt{\tau})$, $u = 1, \ldots, T$, *respectively, where* $\mathbf{r}_{\cdot j} = (r_{1j}, \ldots, r_{Tj})'$ *is the* $j$*'th eigenvector of* $\mathbf{G}$, $j = 1, \ldots, m$. *Then for any* $\beta \in (0, 1]$ *we have* $\|r_j - \rho_j\|^2 = o_p(1/n^{(1-\beta)/2}) + o(1)$ *and consequently* $r_j(t)$ *converges in probability to* $\rho_j(t)$ *in* $\mathcal{L}^2_{[0,\tau]}$.

These consistency properties indicate that for $(n, T)$ reasonably large the empirical expansion in (5) will provide a close approximation to the theoretical expansion in (1), with the construction of $\mathbb{X}^*$ via (25) mimicking the data generating mechanism for $\mathbb{X}$ . An advantage of the representation in (25) is that it suggests how the raw bootstrap can be readily adapted and modified in order to meet different purposes and allow for different scenarios.

The following adaptation, for example, indicates how we can simulate different realizations of a process whose stochastic structure approximates that of the process giving rise to the original data in $\mathcal{X}$: Simulation Step

S1. As in B1. above;

S2. For $i = 1, \ldots, n$ generate new realizations $u_{ij}^*, j = 1, \ldots, m$, by taking i.i.d. random draws from a standard normal variable;

S3. As in B3. above.

The Karhunen–Loève expansion tells us that the random variation observed in $\mathcal{X}$ emanates from fluctuations in the principle component scores, or equivalently, the random coefficients $\upsilon_j$, $j = 1, 2, \ldots$, in (3). These coefficients constitute an uncorrelated sequence of random variables, each with zero mean and unit variance, and the $u_{ij}\,, j = 1, 2, \ldots, m$, in (5) may be viewed as representing a realization of $n$ values of the $\upsilon_j$. Hence the assignment made in step one, the simple random sampling to produce $u^*_{ij}$, $j = 1, 2, \ldots, m$, in the second step, and the construction used in the third step. The rationale behind generating the $u^*_{ij}$ as independent standard normal variables comes from noting that the matrix $\mathbf{U}$ lies in the Stiefel manifold and a natural distribution to take on this manifold is the Fisher-von Mises distribution. As the concentration parameter increases the Fisher-von Mises distribution can be well approximated by a standard normal distribution.

In order to illustrate these ideas Figure 6 graphs the values of $l_k$, $k = 1, \ldots, m$,

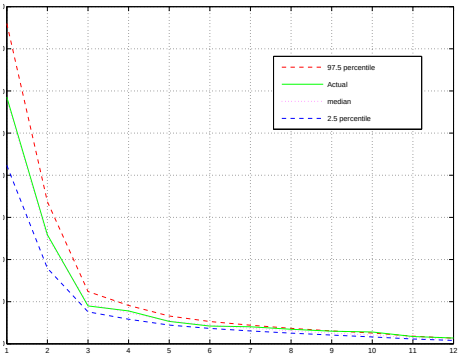


Figure 6: Median value, and 2.5% and 97.5% percentiles, of $l^*_k$ computed from 25000 bootstrap replications derived from the SOI data.

evaluated from the SOI data, together with the 2.5%, 50.0% and 97.5% percentile values of $l^*_k$ computed from 25000 bootstrap replications B1-B3. The fact that the median values of the $l^*_k$ are virtually indistinguishable from the $l_k$ clearly reflects the operation of Lemma 2.

We also computed the empirical distribution of $l^*_k$, $k = 1, \ldots, m$, from 25000 simulated replications S1-S3. Of particular interest from our current perspective is the fact that any differences in the two distributions were not statistically significant, according to a Kolmogorov-Smirnov test, at any conventional significance level. This result lends incidental support to out previous findings concerning the erratic behaviour of the SOI.

Now consider replacing $\mathbb{X}^*$ in (25) by the modified version $\mathbf{s}\bar{\mathbb{X}} + n^{1/2}\mathbf{U}^*\mathbf{L}^*\mathbf{R}'$ where $\mathbf{L}^* = \mathrm{diag}(\sqrt{l_1}, \ldots, \sqrt{l_\kappa}, \sqrt{l^*_{\kappa+1}}, \ldots, \sqrt{l^*_m})$ and $l^*_j = (\delta^*)^2 l_j$, $j = \kappa + 1, \ldots, m$, $\delta^*$ small. This simple modification is designed to mirror the signal-plus-noise structure in (7), when expressed as in (9). Figure 7 presents graphs of the average value of $DL_N(k)$ evaluated from ten modified data sets $\mathbb{X}^*_g$ based upon the OC data. For $g = 1, \ldots, 10$ each $\mathbb{X}^*_g$ was obtained by replacing $\mathbf{L}$ by $\mathbf{L}^*_g = \mathrm{diag}(\sqrt{l_1}, \ldots, \sqrt{l_{25}}, \delta^*_g\sqrt{l_{26}}, \ldots, \delta^*_g\sqrt{l_{216}})$ where $\delta^*_g = (0.8)^{g-1}$. The behaviour predicted in Theorem 3 is clearly apparent in the appearance of the sharply defined minimum in $DL_N(k)$ at $k = \kappa = 25$ as $\delta^*_g$ decreases.

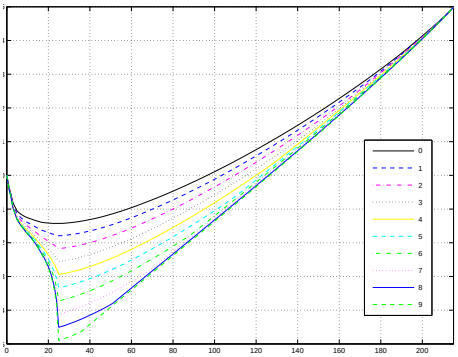

Figure 7: Graphs of $DL_N(k)$ computed from 25000 bootstrap replications of $\mathbb{X}_g^*$ derived from the OC data.

# Appendix: Proofs

Proof of Lemma 1: First observe that, setting $d_u = \frac{1}{n}\sum_{s=1}^{n}\{X_s(t_u) - \mu(t_u)\}$, we have $E[\|\mathbf{d}\|^2] = \sum_{k=1}^{T} E[d_k^2]$. Now, by (12) and (13) of Assumption 2, $E[d_u^2] = n^{-2}Var\left[\sum_{s=1}^{n}\{X_s(t_u) - \mu(t_u)\}\right]$, which we can bound above by

$$2n^{-2}\sum_{s=1}^{n}\sum_{r=0}^{n-s} Cov[X_s(t_u)X_{s+r}(t_u)] \leq 2n^{-1}\sup_s \sum_{r=0}^{\infty} Cov[X_s(t_u)X_{s+r}(t_u)]\,.$$

It now follows from (14) of Assumption 2 that $\sum_{k=1}^{T} E[d_k^2] < 2C_1T/n$.

Similarly, to establish the second part of the lemma note that we have $E[\|\mathbf{D}\|^2] = \sum_{k=1}^{T}\sum_{l=1}^{T} E[D_{kl}^2]$ where, by (12) and (13) of Assumption 2,

$$\begin{aligned} E[D_{kl}^2] &= E\left[\left\{\frac{1}{n}\sum_{s=1}^{n}\{X_s(t_u) - \mu(t_u)\}\{X_s(t_v) - \mu(t_v)\}] - \Gamma(t_u,t_v)\right\}^2\right] \\ &= \frac{1}{n^2}Var\left[\sum_{s=1}^{n}\{X_s(t_u) - \mu(t_u)\}\{X_s(t_v) - \mu(t_v)\}\right]. \end{aligned} \tag{26}$$

Proceeding as previously we can bound the right hand side of equation (26) by $2n\sup_s\sum_{r=0}^{\infty} Cov[\Xi_s(uv)\Xi_{s+r}(uv)]$. From (15) of Assumption 2 we can now deduce that $\sum_{k=1}^{T}\sum_{l=1}^{T} E[D_{kl}^2] < 2C_2T^2/n$, giving the desired result. □

Proof of Lemma 2: Using the inequality $\sum_{j=1}^{m} l_j\ell_j \geq \mathrm{tr}(\mathbf{G}\mathbf{\Gamma}')$ (Anderson and Das-Gupta, 1963) we find that $\sum_{j=1}^{m}(l_j - \ell_j)^2 \leq \|\mathbf{G} - \mathbf{\Gamma}\|^2$, and $\|\mathbf{G} - \mathbf{\Gamma}\|^2$ is $o_p(T^2/n^{(1-\beta)})$ as $n \to \infty$ by Lemma 1, establishing (16).

From (16) we can readily deduce that $\max_{1\leq j\leq m}(l_j - \ell_j)^2 = o_p(T^2/n^{(1-\beta)})$, which implies that the first term on the right hand side of the inequality

$$\max_{1\leq j\leq m}\left|\frac{l_j}{T} - \frac{\lambda_j}{\tau}\right| \leq \max_{1\leq j\leq m}\left|\frac{l_j}{T} - \frac{\ell_j}{T}\right| + \max_{1\leq j\leq m}\left|\frac{\ell_j}{T} - \frac{\lambda_j}{\tau}\right| \tag{27}$$

is $o_p(1/n^{(1-\beta)/2})$. Using arguments that parallel those employed in Hall and Hosseini-Nasab (2006, Theorem 1) it can also be shown that the second term on the right hand side of (27) is $o(1)$. This then establishes (17).

In order to verify (18) of Lemma 2 first observe that $\left|\sum_{j=1}^{m} l_j/T - \sum_{j=1}^{\infty}\lambda_j/\tau\right|$ is bounded above by $\sum_{j=1}^{m}|l_j/T - \lambda_j/\tau| + \sum_{j=m+1}^{\infty}\lambda_j/\tau$. Now, from (17) we have $\max_{1\le j\le m}|l_j/T - \lambda_j/\tau| = o_p(1/n^{(1-\beta)/2}) + o(1)$, and since $\sum_{j=1}^{\infty}\lambda_j$ is a convergent series $\sum_{j=m+1}^{\infty}\lambda_j \to 0$ as $m\to\infty$. It follows therefore that $\sum_{j=1}^{m}|l_j/T - \lambda_j/\tau| \le m\max_{1\le j\le m}|l_j/T - \lambda_j/\tau| = o_p(m/n^{(1-\beta)/2}) + o(m)$ and the proof of the lemma is complete. □

Proof of Lemma 3: Using (17) and (18) of Lemma 2, we obtain for each $k$, $1\le k\le m$,

$$\begin{aligned}\widehat{\pi}_k &= \frac{(mT)^{-1}\sum_{j=1}^{k} l_j}{(mT)^{-1}\sum_{j=1}^{m} l_j}\\ &= \frac{(m\tau)^{-1}\sum_{j=1}^{k}\lambda_j + o_p(k/mn^{(1-\beta)/2}) + o(k/m)}{(m\tau)^{-1}\sum_{j=1}^{\infty}\lambda_j + o_p(1/n^{(1-\beta)/2}) + o(1)}\\ &= \frac{\sum_{j=1}^{k}\lambda_j}{\sum_{j=1}^{\infty}\lambda_j} + \left(\frac{\sum_{j=k+1}^{\infty}\lambda_j}{\sum_{j=1}^{\infty}\lambda_j} + 1\right)\left(o_p(1/n^{(1-\beta)/2}) + o(1)\right). \qquad (28)\end{aligned}$$

From (28) we can conclude that $|\widehat{\pi}_k - \pi_k| \le 2\left(o_p(1/n^{(1-\beta)/2}) + o(1)\right)$, and hence that $|\widehat{\pi}_k - \pi_k| = o_p(1/n^{(1-\beta)/2}) + o(1)$, as required. □

Proof of Theorem 1: That $\widehat{SNR}(k)$ converges to $SNR(k)$ follows from Lemma 3 by Slutky's Theorem. Now presume, for a given $\alpha\in[0,1)$, that $\hat{k}_\alpha > k_\alpha$ for all $n > n'$ and $T > T'$. This implies that $\widehat{SNR}(k_\alpha) \le SNR(\hat{k}_\alpha) + \epsilon$, $\epsilon > 0$, as $(n,T)\to(\infty,\infty)$. Similarly, presuming that $\hat{k}_\alpha < k_\alpha$ for all $n$ and $T$ sufficiently large implies that $\widehat{SNR}(k_\alpha) \ge SNR(\hat{k}_\alpha) - \epsilon$. Thus $|\widehat{SNR}(k_\alpha) - SNR(\hat{k}_\alpha)| \to 0$ as $(n,T)\to(\infty,\infty)$ and hence $\hat{k}_\alpha = k_\alpha$ for $n$ and $T$ sufficiently large. □

Proof of Theorem 2: We know from Lemma 3 that $|\widehat{\pi}_k - \pi_k| = o_p(1/n^{(1-\beta)/2}) + o(1)$. From the expression $\log\left((1-\widehat{\pi}_k)/(1-\pi_k)\right) = \log\left(1 + (\pi_k - \widehat{\pi}_k)/(1-\pi_k)\right)$ and the McLaurin expansion $\log(1+x) = \sum_{r\ge1}(-)^{r-1}x^r/r$ it now follows that $\left|\overline{DL}_2(k) - DL_2(k)\right| = o_p(1/n^{(1-\beta)/2}) + o(1)$, as stated. Similarly,

$$\log\left(\frac{1-\widehat{\pi}_k}{1-\pi_k}\right)\left(\frac{\pi_k}{\widehat{\pi}_k}\right) = \log\left(1 + \frac{\pi_k - \widehat{\pi}_k}{1-\pi_k}\right) - \log\left(1 + \frac{\widehat{\pi}_k - \pi_k}{\pi_k}\right)$$

and using the McLaurin expansion of $\log(1+x)$ once again we can conclude that $\left|\overline{DL}_N(k) - DL_N(k)\right| = o_p(1/n^{(1-\beta)/2}) + o(1)$.

Now presume that $\widetilde{k}_a \ne \overline{k}_a$ for $a\in\{2,N\}$. Then we have

$$DL_a(\widetilde{k}_a) - DL_a(\overline{k}_a) = \left(DL_a(\widetilde{k}_a) - \overline{DL}_a(\widetilde{k}_a)\right) + \left(\overline{DL}_a(\widetilde{k}_a) - \overline{DL}_a(\overline{k}_a)\right). \qquad (29)$$

By definition of $\widetilde{k}_a$ and $\overline{k}_a$ as the minimizing values of $DL_a(k)$ and $\overline{DL}_a(k)$, respectively, the limit-supremum of the left had side of (29) is zero and, given that the first term on the right hand side converges to zero, the limit-infimum of the right hand side is positive. Thus we have the desired result *reductio ad absurdum*. □

Proof of Theorem 3: Consider first $\overline{DL}_N(k)$. Straightforward if somewhat tedious manipulations indicate that we can expand $\overline{DL}_N(k) - \overline{DL}_N(k+1)$ and express it as

the product of $(n+T)/nT$ times

$$\frac{nT}{(n+T)}\log\left(1+\frac{\lambda_{k+1}}{\sum_{j=k+2}^{\infty}\lambda_j}\right)-\log\left(\frac{nT-(k+1)(n+T)}{n+T}\right) \tag{30}$$

$$-\log\left(1+\frac{\lambda_{k+1}}{\sum_{j=1}^{k}\lambda_j}\right)+(k+1)\log\left(\frac{nT-k(n+T)}{nT-(k+1)(n+T)}\right) \tag{31}$$

$$-\log\left(1+\frac{\sum_{j=1}^{k+1}\lambda_j}{\sum_{j=k+2}^{\infty}\lambda_j}\right)+k\log\left(\frac{k+1}{k}\right)+\log(k)\ . \tag{32}$$

When $k<\kappa$ we find from (11) that $\log\left(1+\lambda_{k+1}/\sum_{j=k+2}^{\infty}\lambda_j\right)$ equals

$$\begin{cases}\log\left(1+\frac{\eta_{k+1}+\delta^2\sum_{i=1}^{\infty}\theta_i\beta_{i(k+1)}^2}{\sum_{j=k+2}^{\kappa}\eta_j+\delta^2\sum_{j=k+2}^{\infty}\sum_{i=1}^{\infty}\theta_i\beta_{ij}^2}+O(\delta^2)\right), & \text{when } k\le\kappa-2;\\ \log\left(1+\frac{\eta_{\kappa}+\delta^2\sum_{i=1}^{\infty}\theta_i\beta_{i\kappa}^2}{\delta^2\sum_{j=\kappa+1}^{\infty}\sum_{i=1}^{\infty}\theta_i\beta_{ij}^2}+O(\delta^2)\right), & \text{when } k=\kappa-1.\end{cases}$$

Both of these expressions are positive as $\delta\to 0$, implying that the first term in (30) will dominate all others in the expansion of $\overline{DL}_N(k)-\overline{DL}_N(k+1)$ and thus that $\overline{DL}_N(k)-\overline{DL}_N(k+1)$ will be positive as $(n,T)\to(\infty,\infty)$.

Now suppose that $k\ge\kappa$ and that Assumption 3 obtains. Expression (11) implies that

$$\log\left(1+\frac{\lambda_{k+1}}{\sum_{j=k+2}^{\infty}\lambda_j}\right)=\log\left(1+\frac{\sum_{i=1}^{\infty}\theta_i\beta_{i(k+1)}^2}{\sum_{j=k+2}^{\infty}\sum_{i=1}^{\infty}\theta_i\beta_{ij}^2}+O(\delta^2)\right).$$

By Assumption 3 $\sum_{j=k+2}^{\infty}\sum_{i=1}^{\infty}\theta_i\beta_{ij}^2>\delta^{d-2}(C\sum_{i=1}^{\infty}\theta_i-\delta^{2-d}\sum_{j=1}^{k+1}\sum_{i=1}^{\infty}\theta_i\beta_{ij}^2)>\delta^{d-2}(C-\delta^{2-d})\sum_{i=1}^{\infty}\theta_i=\delta^{d-2}C'$, say. We can therefore conclude that the limit-supremum of the two terms in (30) will not exceed a figure that is of magnitude $(nT/(n+T))\,O(\delta^{2-d})-\log(nT/(n+T))$ . We also find that

$$\log\left(1+\frac{\lambda_{k+1}}{\sum_{j=1}^{k}\lambda_j}\right)=\log\left(1+\frac{\delta^2\sum_{i=1}^{\infty}\theta_i\beta_{i(k+1)}^2}{\sum_{j=1}^{\kappa}\eta_j+\delta^2\sum_{j=1}^{k}\sum_{i=1}^{\infty}\theta_i\beta_{ij}^2}+O(\delta^2)\right),$$

and the two terms in (31) will be of order $-O(\delta^2)+(k+1)o(1)$, and that

$$\log\left(1+\frac{\sum_{j=1}^{k+1}\lambda_j}{\sum_{j=k+2}^{\infty}\lambda_j}\right)=\log\left(1+\frac{\sum_{j=1}^{\kappa}\eta_j+\delta^2\sum_{j=1}^{k+1}\sum_{i=1}^{\infty}\theta_i\beta_{ij}^2}{\delta^2\sum_{j=k+2}^{\infty}\sum_{i=1}^{\infty}\theta_i\beta_{ij}^2}+O(\delta^2)\right),$$

and the two terms in (32) will be of order $-O(\delta^{-2})+O(k)$. Adding the six terms in (30), (31) and (32) together now leads to the conclusion that when $k\ge\kappa$, $\overline{DL}_N(k)-\overline{DL}_N(k+1)$ will be negative as $\delta\to 0$, provided that $\delta^{2-d}nT/(n+T)\to 0$ as $(n,T)\to(\infty,\infty)$.

Parallel but less complicated arguments also show that: (i) $\overline{DL}_2(k)$ is monotonically decreasing in $k$ for $k<\kappa$; and (ii) $\overline{DL}_2(k)$ is monotonically increasing in $k$ for $k\ge\kappa$ when Assumption 3 holds and $\delta^{2-d}nT/(n+T)\to 0$.

Thus, for both $a\in\{2,N\}$ we can conclude that $\overline{k}_a\ge\kappa$, and that $\overline{k}_a=\kappa$ when Assumption 3 holds and $\delta^{2-d}nT/(n+T)\to 0$. The properties stated in the theorem now follow directly from Theorem 2. □

Proof of Lemma 4: Set $\bar{\Gamma}(t,s) = (\tau/T)\sum_{j=1}^{m} l_j r_j(t) r_j(s)$. Using Bosq (2000, Lemma 4.3) we can deduce, as in the proof of their Theorem 1 by Hall and Hosseini-Nasab (2006), that $\|r_j - \rho_j\|^2 \leq 3\Delta/d^2$ where $d = \min_{1\leq j\leq m}(\lambda_j - \lambda_{j+1})$ and $\Delta = \int_0^\tau \int_0^\tau |\bar{\Gamma}(t,s) - \Gamma(t,s)|^2 dtds$. Replacing the integrals by their approximating sums we have $\Delta \leq (\tau^2/T^2)\sum_{u=1}^{T}\sum_{v=1}^{T} |\bar{\Gamma}(t_u,t_v) - \Gamma(t_u,t_v)|^2 + o(1) = (\tau^2/T^2)\|\mathbf{G} - \mathbf{\Gamma}\|^2 + o(1)$. By Lemma 1 $\|\mathbf{G} - \mathbf{\Gamma}\|^2 = o_p(T^2/n^{1-\beta})$, and the proof is thereby completed. □

# References


Anderson, T. W. and S. Das-Gupta (1963). Some inequalities on characteristic roots of matrices. *Biometrika 50*, 522–524.

Banks, D. (2003). Proteomics: A frontier between genomics and metabolomics. *Chance 16*, 6–7.

Bosq, D. (2000). *Linear Processes in Function Spaces: Theory and Applications.* Lecture Notes in Statistics, Springer, New York.

Chiou, Jeng-Min and Li, Pai-Ling (2007) Functional clustering and identifying substructures of longitudinal data. *Journal of the Royal Statistical Society: Series B (Statistical Methodology) 69*(4), 679–699.

Ferraty, F. and P. Vieu (2003). Curve discrimination: A nonparametric functional approach. *Computational Statistics and Data Analysis 44*, 161–173.

Ferraty, F. and P. Vieu (2006). *Nonparametric Functional Data Analysis: Theory and Practice*. Springer, New York.

Grünwald, P. D. (2007). *The Minimum Description Length Principle*. The MIT Press, Cambridge.

Hall, P. and M. Hosseini-Nasab (2006). On properties of functional principal components analysis. *Journal of the Royal Statistical Society: Series B (Statistical Methodology) 68*(1), 109–126.

Hall, P., H.-G. Muller, and J.-L. Wang (2006). Properties of principal component methods for functional and longitudinal data analysis. *The Annals of Statistics 34*, 1493–1517.

Hall, P., D. S. Poskitt, and B. Presnell (2001, feb). A functional data-analytic approach to signal discrimination. *Technometrics 43*(1), 1–9.

Hall, P. and C. Vial (2006). Assessing the finite dimensionality of functional data. *Journal of the Royal Statistical Society: Series B (Statistical Methodology) 68*(4), 689–705.

Hansen, M. and B. Yu (2001). Model selection and the principle of minimum description length. *Journal of the American Statistical Association 96*, 746–774.

Jolliffe, I. T. (2002). *Principal Component Analysis*. Springer, New York.

Ramsay, J. O. and B. W. Silverman (1997). *Functional Data Analysis*. Springer, New York.

Ramsay, J. O. and B. W. Silverman (2002). *Applied Functional Data Analysis Methods and Case Studies*. Springer, New York.

Rissanen, J. (2000). MDL denoising. *IEEE Transactions on Information Theory IT-46*, 2537–2543.

Rissanen, J. (2007). *Information and complexity in statistical modeling*. Springer, New York.

Schwarz, G. (1978). Estimating the dimension of a model. *Annals of Statistics 6*, 461–464.

Shibata, R. (1981). An optimal selection of regression variables. *Biometrika 68*, 45–54.

Stone, R., I. Smith, and P. McIntosh (2000). *Statistical Methods for Deriving Seasonal Climate Forecasts From GCM's*, Chapter 10,Applications of Seasonal Climate Forecasting in Agricultural and Natural Ecosystems, pp. 135–147. Kluwer Acedemic.

Thiele, H. (2003). Proteomics: Mass spectrometry and bioinformatics in proteomics. *Chance 16*, 29–36.

Yao, F., H. G. Muller, and J. L. Wang (2005). Functional data analysis for sparse longitudinal data. *Journal of American Statistical Association 100*, 577–590.

# Supplement: Description Length and Dimensionality Reduction in Functional Data Analysis

Proof of Lemma 2: In the proof of Lemma 2 it is stated that arguments that parallel those surrounding Theorem 1 of Hall and Hosseini-Nasab (2006) can be used to show that the second term on the right hand side of (27) is $o(1)$. The detailed steps, which are long and rather arduous, are presented in this supplement.

We will show that $\max_{1\leq j\leq m}|\ell_j/T-\lambda_j/\tau| = o(1)$ by induction. To this end, let $f_j(t)$ be interpolating cubic smoothing splines that pass through the knots $(t_u, \sqrt{T}e_{uj}/\sqrt{\tau})$, $u=1,\ldots,T$, respectively, where $\mathbf{e}_j = (e_{1j},\ldots,e_{Tj})'$ is the j'th eigenvector of $\mathbf{\Gamma}$. Then by definition $\frac{\tau}{T}\sum_{u=1}^{T} f_j(t_u)^2 = 1$ and we have

$$\sum_{v=1}^{T}\Gamma(t_u,t_v)f_j(t_v) = \ell_j f_j(t_u) \tag{33}$$

and

$$\frac{\tau}{T^2}\sum_{u=1}^{T}\sum_{v=1}^{T} f_j(t_u)\Gamma(t_u,t_v)f_j(t_v) = \frac{\ell_j}{T}\,. \tag{34}$$

Similarly, $\lim_{T\to\infty}\tau/T\sum_{u=1}^{T}\rho_j(t_u)^2 = \int_0^\tau \rho_j(t)^2dt = 1$, and as $T\to\infty$

$$\frac{\tau}{T}\sum_{v=1}^{T}\Gamma(t_u,t_v)\rho_j(t_v) \to \int_0^\tau \Gamma(t_u,t)\rho_j(t)dt = \lambda_j\rho_j(t_u) \tag{35}$$

and

$$\begin{aligned}\frac{\tau^2}{T^2}\sum_{u=1}^{T}\sum_{v=1}^{T}\rho_j(t_u)\Gamma(t_u,t_v)\rho_j(t_v) &\to \int_0^\tau\int_0^\tau \rho_j(t)\Gamma(t,s)\rho_j(s)dtds \\ &= \lambda_j\,. \end{aligned}\tag{36}$$

Starting at $j=1$, we can conclude from (34) that

$$\left|\frac{\ell_1}{T} - \frac{1}{\tau}\int_0^\tau\int_0^\tau f_1(t)\Gamma(t,s)f_1(s)dtds\right| \to 0 \tag{37}$$

as $T\to\infty$, and hence that $\limsup_{T\to\infty}(\ell_1/T-\lambda_1/\tau)\leq 0$ since the double integral in (37) is bounded above by $\lambda_1$. By the Rayleigh-Ritz Theorem

$$\begin{aligned}&\frac{\tau^2}{T^2}\sum_{u=1}^{T}\sum_{v=1}^{T}\rho_1(t_u)\Gamma(t_u,t_v)\rho_1(t_v) \\ &\qquad= \frac{\tau}{T}\left(\frac{\sum_{u=1}^{T}\sum_{v=1}^{T}\rho_1(t_u)\Gamma(t_u,t_v)\rho_1(t_v)}{\sum_{u=1}^{T}\rho_1(t_u)^2}\right)\left(\frac{\tau}{T}\sum_{u=1}^{T}\rho_1(t_u)^2\right) \\ &\qquad\leq \left(\frac{\tau}{T}\right)\ell_1\left(\frac{\tau}{T}\sum_{u=1}^{T}\rho_1(t_u)^2\right)\,,\end{aligned}$$

which implies, via (36), that the $\liminf_{T\to\infty}(\ell_1/T-\lambda_1/\tau)\geq 0$. From the inequalities $\limsup_{T\to\infty}(\ell_1/T-\lambda_1/\tau)\leq 0$ and $\liminf_{T\to\infty}(\ell_1/T-\lambda_1/\tau)\geq 0$ we can conclude that $|\ell_1/T-\lambda_1/\tau|\to 0$ as $T\to\infty$.

Suppose now that $\max_{j=1,\ldots,(k-1)} |\ell_j/T - \lambda_j/\tau| \to 0$ as $T \to \infty$. Equations (33) for $j = 1, \ldots, (k-1)$ and (35) for $j = k$ imply that

$$\lim_{T\to\infty} \left| \left( \frac{\ell_j}{T} - \frac{\lambda_k}{\tau} \right) \frac{\tau}{T} \sum_{u=1}^{T} f_j(t_u)\rho_k(t_u) \right| = 0\,,$$

and since

$$0 < \left| \frac{\lambda_j}{\tau} - \frac{\lambda_k}{\tau} \right| \leq \left| \frac{\lambda_j}{\tau} - \frac{\ell_j}{T} \right| + \left| \frac{\ell_j}{T} - \frac{\lambda_k}{\tau} \right|$$

and by assumption $|\ell_j/T - \lambda_j/\tau| = o(1)$, it follows that

$$\lim_{T\to\infty} |\frac{\tau}{T} \sum_{u=1}^{T} f_j(t_u)\rho_k(t_u)| = 0\,. \tag{38}$$

Thus $\rho_k(t)$ is asymptotically orthogonal to $f_j(t)$, $j = 1, \ldots, (k-1)$. Set $\rho_k(t) = \widehat{\rho}_k(t) + \varrho_k(t)$ where

$$\widehat{\rho}_k(t) = \sum_{j=1}^{(k-1)} f_j(t) \left( \frac{\tau}{T} \sum_{u=1}^{T} f_j(t_u)\rho_k(t_u) \right)\,.$$

From the Cauchy-Schwartz inequality we have

$$\frac{\tau^2}{T^2} \sum_{u=1}^{T} \sum_{v=1}^{T} \rho_k(t_u)\Gamma(t_u, t_v)\rho_k(t_v) \leq (\widehat{s}_k + s_k)^2$$

where

$$\widehat{s}_k^2 = \frac{\tau^2}{T^2} \sum_{u=1}^{T} \sum_{v=1}^{T} \widehat{\rho}_k(t_u)\Gamma(t_u, t_v)\widehat{\rho}_k(t_v) = \sum_{j=1}^{(k-1)} \ell_j \left( \frac{\tau}{T} \sum_{u=1}^{T} f_j(t_u)\rho_k(t_u) \right)^2$$

and, by the Courant-Fischer Theorem,

$$s_k^2 = \frac{\tau^2}{T^2} \sum_{u=1}^{T} \sum_{v=1}^{T} \varrho_k(t_u)\Gamma(t_u, t_v)\varrho_k(t_v) \leq \left( \frac{\tau}{T}\ell_k \right) \left( \frac{\tau}{T} \sum_{u=1}^{T} \varrho_k(t_u)^2 \right)\,.$$

Thus

$$\frac{\tau^2}{T^2} \sum_{u=1}^{T} \sum_{v=1}^{T} \rho_k(t_u)\Gamma(t_u, t_v)\rho_k(t_v) \leq \left( \left( \frac{\tau}{T}\ell_k \right) + \Delta\ell_k \right) \left( \frac{\tau}{T} \sum_{u=1}^{T} \rho_k(t_u)^2 \right)$$

where

$$\Delta\ell_k = 2 \left( \frac{\tau\ell_k}{T} \frac{\widehat{s}_k^2}{(\tau/T)\sum_{u=1}^{T} \rho_k(t_u)^2} \right)^{1/2} + \frac{\widehat{s}_k^2}{(\tau/T)\sum_{u=1}^{T} \rho_k(t_u)^2}\,.$$

Since $\widehat{s}_k^2 = o(1)$ by virtue of (38) and

$$\frac{\tau\ell_k}{T} < \frac{\tau}{T} \sum_{u=1}^{T} \mathbf{\Gamma}(t_u, t_u) \to \int_0^\infty \Gamma(t, t)dt = \sum_{j=1}^{\infty} \lambda_j < \infty$$

we can conclude via (36) that $\liminf_{m\to\infty}(\ell_k/T - \lambda_k/\tau) \geq -\Delta\ell_k/\tau$ where $\Delta\ell_k \to 0$ as $T \to \infty$.

Replacing $\rho_k(t)$ by $f_k(t)$ and interchanging the role of $f_j(t)$ and $\rho_j(t)$, $j = 1, \ldots, (k-1)$, set $f_k(t) = \widehat{f}_k(t) + \varphi(t)$ where

$$\widehat{f}_k(t) = \sum_{j=1}^{(k-1)} \rho_j(t) < \rho_j, f_k > \ .$$

Then

$$\int_0^\infty \int_0^\infty f_k(t)\Gamma(t,s)f_k(s)dtds \leq (\widehat{\sigma}_k + \sigma_k)^2$$

where

$$\widehat{\sigma}_k^2 = \int_0^\infty \int_0^\infty \widehat{f}_k(t)\Gamma(t,s)\widehat{f}_k(s)dtds = \sum_{j=1}^{(k-1)} \lambda_j < \rho_j, f_k >^2$$

and

$$\sigma_k^2 = \int_0^\infty \int_0^\infty \varphi_k(t)\Gamma(t,s)\varphi_k(s)dtds \leq \lambda_k \, .$$

It follows that as $T \to \infty$

$$\begin{aligned} \frac{\ell_k}{T} &= \frac{\tau}{T^2} \sum_{u=1}^{T} \sum_{v=1}^{T} f_k(t_u)\Gamma(t_u, t_v)f_k(t_v) \\ &\to \frac{1}{\tau} \int_0^\tau \int_0^\tau f_k(t)\Gamma(t,s)f_k(s)dtds \\ &\leq \frac{1}{\tau} \left(\lambda_k + \Delta\lambda_k\right) \, , \end{aligned}$$

where

$$\Delta\lambda_k = 2\widehat{\sigma}_k\sqrt{\lambda_k} + \widehat{\sigma}_k^2 \, .$$

This implies that the $\limsup_{m\to\infty}(\ell_k/m - \lambda_k/\tau) \leq \Delta\lambda_k/\tau$.

Replacing $\rho_k(t)$ by $f_k(t)$ and $f_j(t)$ by $\rho_j(t)$, $j = 1, \ldots, (k-1)$, we can implement an argument parallel to that leading to (38), using equations (33) for $j = k$ and (35) for $j = 1, \ldots, (k-1)$, to show that $f_k(t)$ is asymptotically orthogonal to $\rho_j(t)$, $j = 1, \ldots, (k-1)$, that is,

$$\begin{aligned} | < \rho_j, f_k > | \leq & \\ & | \int_0^\tau f_k(t)\rho_j(t)dt - \frac{\tau}{T} \sum_{u=1}^{T} f_k(t_u)\rho_j(t_u)| + |\frac{\tau}{T} \sum_{u=1}^{T} f_k(t_u)\rho_j(t_u)| \\ & \to 0 \, . \end{aligned}$$

Hence we can conclude that $\widehat{\sigma}_k^2 \to 0$ and thus that $\Delta\lambda_k \to 0$ as $T \to \infty$.

The structure of the limit-infimum and the limit-supremum allows us to conclude that $|\ell_k/m - \lambda_k/\tau| \to 0$ as $T \to \infty$ and hence that

$$\max_{j=1,\ldots,k} |\ell_j/T - \lambda_j/\tau| = \max\{ \max_{j=1,\ldots,(k-1)} |\ell_j/T - \lambda_j/\tau| \, , |\ell_k/T - \lambda_k/\tau| \} = o(1) \, ,$$

completing the induction and thereby the proof of (17).